Published in final edited form as:
Anat Rec (Hoboken). 2012 July ; 295(7): 1192–1201. doi:10.1002/ar.22505.

DIFFERENTIAL DISTRIBUTION PATTERNS FROM MEDIAL PREFRONTAL CORTEX AND DORSAL RAPHE TO THE LOCUS COERULEUS IN RATS

Yuefeng Lu[1], **Kimberly L. Simpson**[1,2], **Kristin J. Weaver**[3], and **Rick C.S. Lin.**[1,2]

[1]Department of Neurobiology and Anatomical Science, University of Mississippi Medical Center, Jackson, MS 39216.

[2]Department of Psychiatry and Human Behavior, University of Mississippi Medical Center, Jackson, MS 39216.

[3]Department of Neurosurgery, University of Florida, Gainesville, FL 32610.

Abstract

Locus coeruleus (LC) consists of a densely packed nuclear core and a surrounding plexus of dendritic zone which is further divided into several sub-regions. Whereas many limbic-related structures topographically target specific sub-regions of the LC, the precise projections from two limbic areas, i.e., medial prefrontal cortex (mPFC) and dorsal raphe (DR), have not been investigated. The goal of the present study is to identify and compare the distribution patterns of mPFC and DR afferent terminals to the LC nuclear core as opposed to specific pericoerulear dendritic regions (Peri-LC). To address these issues, anterograde tracer injections were combined with dopamine-β-hydroxylase (DBH) immunofluorescent staining in order to reveal the distribution patterns around the LC nuclear complex. Our data suggest that both mPFC-LC and DR-LC projections exhibit selective afferent terminal patterns. More specifically, mPFC-LC projecting fibers mainly target the rostromedial Peri-LC, whereas DR-LC projecting fibers demonstrate a preference to the caudal juxtaependymal Peri-LC. Thus, our present findings provide further evidences that afferents to the LC are topographically organized. Understanding the relationship among different inputs to the LC may help to elucidate the organizing principle which likely governs the interactions between the broad afferent sources of the LC and its global efferent targets.

Keywords

Medial prefrontal cortex; Dorsal raphe; Locus coeruleus; Serotonin; Norepinephrine

INTRODUCTION

LC nucleus is well known for its extensive noradrenergic projections from the spinal cord to the neocortex (Swanson and Hartman, 1975; Foote et al., 1983). It gives rise to more than 90% of the norepinephrine (NE) innervations of the central nervous system (CNS) and is the sole source of NE projection to the cortex and the hippocampus (Swanson 1976a; Barnes and Pompeiano, 1991). Anatomically, LC is composed of a densely packed nuclear core and a surrounding noradrenergic process zone which is asymmetrically distributed and contains

Corresponding Author: Rick C.S. Lin Departments of Neurobiology and Anatomical Science, Psychiatry and Human Behavior University of Mississippi Medical Center Jackson, MS 39216 Tel: (601) 984-1665 Fax: (601) 984-1655 rlin@anatomy.umsmed.edu.

mostly dendrites. These extranuclear dendrites extend preferentially into two distinct Peri-LC regions: the rostromedial and caudal juxtaependymal Peri-LC (Shipley et al., 1996). Furthermore, these extranuclear LC dendrites are important sites for input integration in that each dendrite is contacted by several presynaptic terminals but never presynaptic to other structures (Shipley et al., 1996).

In spite of its broad projection, neurons in LC are not homogenous (for review: Foote et al., 1983). For example, while LC projection to whisker-related cortical area is known to be mainly ipsilateral, the projection to whisker-related sub-cortical area shows bilateral pattern (Simpson et al., 1997). In addition, forebrain projecting LC neurons are more rostrally located (Swanson. 1976 a and b) than spinal cord projecting LC neurons (Clark and Proudfit, 1991; Proudfit and Clark, 1991). On the other hand, the topographic architecture from diverse sources to the LC has also been noticed (Aston-Jones et al., 1986; Luppi et al., 1995; Valentino et al., 1996; Van Bockstaele et al., 1999, 2001). For example, nucleus paragigantocellularis (PGI), the major glutamate afferent to the LC, and Barrington's nucleus, a corticotropin-releasing factor (CRF) source of the LC, target only the nuclear core of the LC (Aston-Jones et al., 1986; Valentino et al., 1996). In contrast, the central nucleus of the amygdala (CNA) and the bed nucleus of the stria terminalis (BNST), two major CRF afferents to the LC (Van Bockstaele et al., 2001), send afferent fibers mainly to the rostrolateral Peri-LC (Ennis et al., 1991). Finally, the ventrolateral part of the periaqueductal gray area (PAG) sends its afferent fibers mainly to the rostromedial Peri-LC (Ennis et al., 1991). These studies suggest selective afferent patterns to the LC, and further implicate that different inputs to the LC may selectively modulate specific subpopulation of neurons in the LC.

Both mPFC and DR are known to play important roles in stress (Amat et al., 2005). In particular, mPFC has been regarded as the cognitive center of the cortex and regulates the hypothalamo-pituitary-adrenal axis response. (Amodio and Frith, 2006; Radley et al., 2006). On the other hand, DR, the major serotonergic nucleus in the brainstem, is recognized as the most important nucleus in stress-related mental disorders (Blier and DE Montigny, 1997; Owens and Nemeroff, 1994; Ressler and Nemeroff, 2000). Anatomically, previous retrograde studies have demonstrated the projections from mPFC and DR to the LC (Cedarbaum and Aghajanian, 1978; Imai et al., 1986; Luppi et al., 1995; Kim et al., 2004; Lee et al., 2005), and anterograde tracing studies have demonstrated the afferent terminals from these two areas (Sesack et al; 1989; Vertes and Kocsis, 1994). Unfortunately, the precise location of terminals from these two sources to the LC nuclear core vs specific Peri-LC areas has yet to be elucidated.

In the present study, anterogradely labeled fibers from mPFC and DR were combined with dopamine-β-hydroxylase (DBH) immunohistochemistry in order to reveal the precise topographic relationship between afferent terminals and the DBH immunoreactive profiles in the LC.

MATERIALS AND METHODS

Subjects

A total of 14 Long-Evans hooded rats weighting 250-300 g were used for the present study. All animals were treated according to guidelines approved by the Institutional Animal Care and Use Committee and conformed to NIH standards for the care and use of animals in research.

Surgery and Tracer Injection

Animals were anesthetized by intraperitoneal administration of Nembutal (50mg/kg). Subjects were then positioned in a stereotaxic apparatus so that the bregma and lambda suture marks were oriented in the horizontal plane. The skull above the mPFC (n=6) or DR (n=8) was removed and tracers were deposited. Coordinates for the placement of tracer agents were derived from the atlas of Paxinos and Watson (1986) and were as follows: mPFC [AP: +2.0 to +3.5 mm; ML: 0.8 mm; VD: 3.0-4.5 mm (from the pia surface)]; and DR [AP: -7.5 to -8.5 mm; ML: 0 to 0.2 mm; VD: 5.5 to 6.0 mm (from the surface of the confluent sinus)]. More specifically for DR injections, anterograde tracers were placed in the caudal part of the DR since DR projections to the LC are mainly originated from caudal part (Kim et al., 2004) and pronounced DR-LC projecting fibers are noted after anterograde tracers were deposited in the caudal part of the DR (Imai et al., 1986; Vertes and Kocsis, 1994). Tryptophan hydroxylase (TPH) immunostaining was used to identify the serotonergic DR neurons, and cases with restricted tracer injections in target areas were used for further analysis (5/6 for mPFC injections and 6/8 for DR injections). Tracing materials employed including biotinylated dextran amine (BDA; 10% in distilled water, Molecular Probes, Eugene, OR) and Fluoro-ruby (FR; 10% in distilled water, Molecular Probes, Eugene, OR). A 10 μl Hamilton syringe containing 0.4/1.0 μl (0.4 μl for DR injections and 1.0 μl for mPFC injections) of tracer was used to mechanically inject over a period of 15-30 minutes.

After a survival period of 7-14 days (7 days for BDA and 14 days for FR), animals were deeply sedated with Nembutal (100 mg/kg) and perfused through the ascending aorta with saline followed by 3.5% paraformaldehyde in 0.1 M phosphate-buffered saline (PBS). Brains were removed immediately and stored at 4 °C overnight in the same fixative with 25% sucrose. The next day, brains were sectioned on a freezing microtome to a thickness of 40 μm.

Immunofluorescent Staining

The reasons for choosing DBH rather than tyrosine hydroxylase (TH) to reveal LC profiles were: 1) DBH, the final enzyme in the biosynthesis of NE (Hartman et al., 1972), specifically identifies NE profiles; 2) TH, the rate-limiting enzyme in catecholamine synthesis (Hartman et al., 1972), labels not only NE in the LC but also dopamine positive profiles in the substantia nigra (SN) and the ventral tegmental area (VTA); and 3) VTA, one of the major dopamine nuclei, has been shown to send dopamine positive terminals to the LC (McRae-Deguerce and Milon, 1983). Thus, DBH staining was chosen to reveal noradrenergic LC profiles instead of TH staining, even though TH staining has been routinely used previously to label LC neurons and their dendrites (Luppi et al., 1995; Valentino et al., 1996; Van Bockstaele et al., 2001).

In order to examine and compare TH and DBH immunostaining patterns in LC, every other sections in LC (40 μm apart) were processed for either monoclonal TH or monoclonal DBH antisera. To visualize TH or DBH immunoreactive profiles, tissues were incubated overnight in TH (1:1000; MAB5280; Millipore) or DBH (1: 1000; MAB394; Millipore) antiserum at 4 °C in PBS with 0.3% Triton X-100 and 1% bovine serum albumin (BSA). The sections were rinsed in PBS the next day and then linked to anti-mouse IgG (1:200; Jackson ImmunoResearch) for 1 hour at room temperature, and finally linked to either streptavidin Cy-2 or Cy-3 (1:200; Jackson ImmunoReserach Lab.) for 1 hour at room temperature.

To visualize anterogradely BDA-labeled projecting fibers, sections were incubated for 1 hour with either streptavidin conjugated Cy-2 or Cy-3 at room temperature. In order to study the exact location of anterogradely labeled projecting fibers around LC, tissues were further processed for DBH immunohistochecistry. In particular, after BDA staining, sections

containing LC were further incubated overnight in DBH antiserum at 4 °C in PBS with 0.3% Triton X-100 and 1% BSA, then exposed to anti-mouse Cy-2 or Cy-3. Colors were coded in a complementary fashion, so that a red fluorophore representing BDA-containing fibers and a green fluorophore revealing DBH profiles, or vice versa. For FR injection cases, the corresponding DBH staining was always labeled with green flurophore, since FR is a fluorescent tracer pre-linked with red flurophore.

To identify DR-LC projecting pattern, the following two staining combinations were employed. 1). Anti-rabbit serotonin transporter (1: 1000; a gift from Dr Zhou, Indiana University; Zhou et al., 1996; Xu et al., 2004; and 1:2000; #20080; ImmunoStar) and DBH antisera of double immunostaining approaches were conducted in order to demonstrate the distribution pattern of SERT positive fibers within the confine of LC. 2). Anterograde BDA tracer injection from DR was combined with DBH immunostaining to examine the distribution pattern of DR-LC projecting fibers in the LC. For SERT immunostaining, tissue was incubated overnight in SERT antiserum (1:1000) at 4 °C in PBS with 0.3% Triton X-100 and 1% BSA, and then linked to either Cy-2 or Cy-3 in a complementary fashion with DBH immuno-staining.

After staining processes, tissues were mounted on gelatin-coated slides and air dried. Slides were then coverslipped with DPX and examined with a fluorescent microscope.

Data analysis and Semi-quantitative assessment

A Nikon epifluorescent microscope (E800) equipped with appropriate filters was used to examine injection sites, labeled fibers, and LC nuclear core vs Peri-LC dendritic areas. Only cases which had injections restricted to the anatomical boundaries of the target area were accepted for further evaluation. To conduct such analysis, every third sections through the LC were placed in a serial order and then examined. Photomicrographs were taken with a Photometrics Coolsnap ES CCD camera (Roper Scientific) and analyzed with a Metamorph imaging software (Universal Imaging Systems). Furthermore, line drawings were made to illustrate rostral, intermediate, and caudal levels of the LC. More specifically, the precise location of projecting fibers at different levels of the LC was plotted and examined in order to reveal the spatial relationship between the afferent terminals and LC noradrenergic profiles.

For the semi-quantification of BDA labeled afferent fiber density within each sub-region of the LC (n=3 for mPFC study; and n=3 for DR study), digitized photomicrographs of selective sections were taken at a magnification of 40x (yielding a field that measured 250 μm of diameter) with same exposing time (10 ms for Cy-3 and 100 ms for Cy-2) for each cases. For a given case, equal numbers of sections (4-6; rostral vs caudal LC levels) were used and analyzed. Typically, 3 images were taken from each sites and then averaged. Metamorph imaging software program (Universal Imaging Systems) was used following previously published procedures (Maciag et al., 2006; Weaver et al., 2010). In particular, images were first “flattened/skeletonized” to distinguish objects of interest from background distortions. A “thresholding” overlay was then applied to each image to delineate regions of interest. This utility specified which information was to be extracted for measurement consideration. In the analysis of fiber density, a region of interest was delineated (20 X 50 μm) using similar sites in different cases. Then, the “percentage of thresholded area” within that region was determined. This measurement referred to the proportion of afferent terminals that was thresholded. Average values from each region were tabulated across cases and recorded as mean values for specific LC nuclear core or Peri-LC dendritic areas. More specifically, the densities of afferent terminals from mPFC and DR to the rostromedial Peri-LC, rostral LC nuclear core, caudal juxtaependymal Peri-LC and caudal LC nuclear core sub-regions were measured and compared. Areas with the highest value of afferent terminal

density were set as 100% and compared to regions with fewer values. Paired student's t-test was used for the comparison, and P value less than 0.05 was considered to be significant.

RESULTS

1. Comparison between DBH and TH immunostaining in LC

In order to reveal the DBH immunostaining pattern in the LC, adjacent DBH and TH immunostained sections were used for comparing (n=4). In coronal sections, DBH and TH immunostainings exhibited rather similar dendritic profiles within the rostromedial and caudal juxtaependymal Peri-LC (Fig.1; B-E). This selective dendritic arrangement was also clearly revealed in horizontal sections (Fig. 1A). DBH labeled dendritic processes extended mainly rostromedially and this sub-area was defined as the rostromedial Peri-LC. In addition, a thin band of noradrenergic processes could also be clearly appreciated between the LC nuclear core and the lateral wall of the IVth ventricle in the caudal medial portion of Peri-LC. This sub-area has been termed as caudal juxtaependymal Peri-LC (Shipley et al., 1996). Since TH staining labels extensive dopaminergic profiles in the VTA and VTA has been shown to provide dopaminergic terminals to the LC (McRae-Deguerce and Milon, 1983), therefore, DBH immunohistochemistry was chosen to reveal the noradrenergic LC profiles in the present study.

2. mPFC preferentially targeting the rostromedial Peri-LC

Either BDA or FR was injected into one side of the mPFC (n=6; 3 animals for each), and similar pattern was observed from these two different tracers. The tracer spread was restricted in the mPFC (Fig. 2), and anterogradely labeled fibers were noted in the ipsilateral LC (Fig. 3). A majority of these labeled fibers were observed at the rostral one-third of the LC and many of them located within the rostromedial Peri-LC sub-region. In addition, a few fibers were found at both intermediate and caudal levels. A few retrogradely labeled LC-mPFC projecting neurons were also noted throughout all levels of LC. Schematic line drawings illustrating the spatial relationship of mPFC afferents to the LC nuclear core vs Peri-LC are shown in Figure 4. The data clearly demonstrate mPFC afferents preferentially targeting rostral LC. To further define this pattern, semi-quantitative analysis was performed to reveal fiber density in different sub-regions. The mean values and standard deviations of mPFC-LC afferent terminal densities (percentage of threshold areas) within specific sub-regions are: 6.5 ± 0.52 in rostromedial Peri-LC (100%; the highest density); 3.67 ± 0.153 in rostral LC nuclear core (~43% less; $P<0.05$); 1.37 ± 0.306 in caudal juxtaependymal Peri-LC (~78% less; $P<0.05$); 1.27 ± 0.493 in caudal LC nuclear core (~80% less; $P<0.05$). Thus, it is quite obvious that rostral LC, especially the rostromedial Peri-LC, contains the highest density of mPFC-LC inputs.

3. DR preferentially targeting the caudal juxtaependymal Peri-LC

Since DR provides most serotonergic fibers to the LC, sections around LC nucleus were processed for both SERT and DBH immunohistochemistry in order to reveal the spatial relationship between serotonergic fibers and LC nuclear core vs Peri-LC (n=4). Our data revealed that SERT positive fibers were prevalent at all levels of the LC, and the most intensely SERT labeled area was restricted to the Peri-LC, especially the caudal juxtaependymal Peri-LC (Fig. 5). In order to further demonstrate that DR-LC afferent terminals were also preferentially targeting the caudal juxtaependymal Peri-LC, anterograde tracer (BDA or FR) was injected into the DR (n=8; 4 each). Six out of 8 cases (n=6; 3 each) with tracer confined to the DR were further analyzed. A representative case showing the injection site restricted to DR is shown in Figure 6. The anterogradely labeled DR-LC projecting fibers were found throughout all levels of the LC and most of them were restricted to the Peri-LC (Fig. 7). In particular, a thin band of densely labeled fibers were

noted at the caudal level situated between LC nuclear core and the lateral wall of the IVth ventricle, a region defined previously as the caudal juxtaependymal Peri-LC. To further demonstrate such relationship, representative schematic line drawings are shown in figure 8. In order to further reveal sub-regional density differences, semi-quantitative analysis was conducted (n=3; BDA injected cases). The mean values and standard deviations of DR-LC afferent terminal densities in specific sub-regions are: 6.2 ± 0.95 in caudal juxtaependymal Peri-LC (the highest density; 100%); 2.17 ± 0.05 in rostromedial Peri-LC (~65% less; $P<0.05$); 2.4 ± 0.4 in rostral LC nuclear core (~61% less; $P<0.05$); 1.6 ± 0.285 in caudal LC nuclear core (~74% less; $P<0.05$).

DISCUSSION

The present study was undertaken to enhance our understanding of the organizing principle between the afferent sources and the efferent targets of the LC nucleus. To accomplish this goal, anterograde tracers were combined with DBH immunostaining. This combined strategy permits the identification of spatial relationships between DBH positive profiles with mPFC and DR afferent terminals in the LC. Our data suggest that mPFC-LC afferent terminals prefer the rostromedial Peri-LC, and in contrast, DR-LC afferent terminals exhibit a preference to the caudal juxtaependymal Peri-LC. To our knowledge, the current investigation is the first report to detail the spatial relationship between mPFC and DR afferent terminals with LC nuclear core and Peri-LC. Our study is also the first to semi-quantify the mPFC and DR afferent fiber densities in different sub-regions of the LC.

Technical Considerations

In order to avoid tracer bias, two anterograde tracers (BDA or FR) were used. Since previous studies have suggested that FR also labels non-neuronal perivascular cells in the brain (Nance and Burns, 1990; Vercelli et al., 2000), therefore, only BDA injected cases (n=3) were used for semi-quantification analysis.

In general, a small amount (0.4 μl) of anterograde tracer was injected via Hamilton syringe into the DR in order to restrict the spread of tracers to adjacent structures such as PAG, which is also known to project to LC (Ennis et al., 1991). With such small amounts of tracer injection in DR, anterogradely labeled afferents were noted in the LC. In order to further reveal the sub-regional fiber density differences regarding the afferent terminals to the LC, MetaMorph software program was used to semi-quantify such differences. It is important to note that this approach has been used recently to examine immunoreactive fiber density changes after various types of manipulation (Maciag et al., 2006; Weaver et al., 2010; Zhang et al., 2011).

mPFC Inputs to the LC

The descending mPFC-LC pathway has been reported previously (Sesack et al., 1989). Using iontophoresis to deposit small volumes of Phaseolus vulgaris leucoagglutinin (PHA-L) in different sub-regions of the mPFC in rats, the authors demonstrated a consistent yet minor afferent terminal pattern to the LC. Unfortunately, the precise distribution pattern of this descending pathway to the sub-architectural zone was not addressed. Our current study demonstrates that mPFC-LC afferent terminals preferentially target the rostromedial Peri-LC dendritic zone. Interestingly, previous study has suggested a similar terminal distribution pattern in primates (Arnsten and Goldman-Rakic, 1984). In particular, horseradish peroxidase (HRP) slow release gels were implanted in prefrontal cortex for 48 hours. Anterogradely labeled afferent terminals were found mainly restricted to the rostral levels of LC and the densest labeled fibers were located at the medial side of LC nucleus. Thus, it is very likely that such preference may be a common pattern among different species.

Despite the wide noradrenergic projection from LC to the cortex, mPFC is the only cortical structure projecting back to the LC (Luppi et al., 1996). mPFC in rats has been suggested as a functional homology with the prefrontal cortex in primates (Rosenkilde. 1983; Brown and Bowman, 2002), which is strongly linked to the processing of higher cortical functions such as emotion and cognition (Goldman-Rakic. 1990; Damasio. 1997). Neurons in the mPFC are able to detect whether a stressor is under the organism's control or not in rat models (Amat et al., 2005). It has also been demonstrated that LC neurons can be activated by mPFC stimulation through both NMDA and non-NMDA receptors, and mPFC provides a resting tonic excitatory influence on LC activity (Jodo and Aston-Jones, 1997; Jodo et al., 1998). The preferential mPFC projection to the rostromedial Peri-LC observed in the present study supports the functional homology between the mPFC in rats and the prefrontal cortex in primates. In brief, the descending mPFC pathway may underlie the activation of noradrenergic LC by emotional and external stressors

DR Inputs to the LC

Previous PHA-L and Cholera-toxin B (CTb) anterograde studies have revealed DR projecting fibers in the LC (Aston-Jones et al., 1991; Vertes and Kocsis, 1994; Luppi et al., 1995). These early studies have noticed that anterogradely labeled DR-LC projecting fibers innervate the Peri-LC region more strongly than LC nuclear core. However, the sub-regional innervation pattern in the Peri-LC was not described. One of the reasons for the lack of information is that the subdivision of Peri-LC and its significance was not revealed until later on (Shipley et al., 1996). By semi-quantifying the DR-LC afferent terminals in different sub-regions, our present finding is the first to suggest that DR-LC projecting fibers preferentially target the caudal juxtaependymal Peri-LC.

Although LC-cortical projecting neurons innervate functionally and cytoarchitectonically distinct cortical regions (Loughlin et al., 1982), LC is not homogenous with respect to the origin of the noradrenergic projections in the central nervous system (CNS); instead, it is comprised of distinct subdivisions of noradrenergic neurons (Mason and Fibiger, 1979). For example, forebrain projecting LC neurons are located more rostrally (Swanson. 1976 a and b) than spinal cord projecting LC neurons (Clark and Proudfit, 1991; Proudfit and Clark, 1991). Thus, it is tempting to speculate that DR-LC pathway, which shows a preference to the caudal juxtaependymal Peri-LC, may exert more effects on descending LC-spinal cord projecting neurons. This descending serotonin-containing inhibitory DR-LC pathway has been proposed to modulate the central pain (Segal and Sanderg, 1977; Segal. 1979). Prolonged administration of selective serotonin reuptake inhibitors (SSRI) reduces the spontaneous firing activity of LC neurons (Szabo et al., 1999; Szabo and Blier, 2001). Clinically, SSRI has been used to treat chronic pain diseases such as noncardiac chest pain, irritable bowel syndrome and poststroke pain in patients without depression (Doraiswamy et al., 2006; Shimodozono et al., 2002; Talley. 2006). Thus, the selective preference of DR-LC projection to the caudal juxtaependymal Peri-LC supports its functional role regarding the central pain modulation circuit.

Topographic Organization of Various Afferents to the LC

Since our data demonstrate that cortical afferents to the LC is quite distinctive from subcortical afferent, one obvious question is that “Is there an organization principle among these reported afferents to the LC?” Previous publication from our laboratory summarized an overall topography and neurochemical identity of afferent inputs to the LC nuclear core vs peri-LC region (Simpson and Lin, 2007). A new schematic diagram (Fig. 9) was made to include the new findings. First, nucleus paragigantocellularis (PGi), nucleus prepositus hypoglossi (PrH), the dorsal cap of the paraventricular nucleus of the hypothalamus and the Barrington's nucleus project to the LC nuclear core (Aston-Jones et al., 1986; Rouzade-

Dominguez et al., 2001; Valentino et al., 1996). On the other hand, many brain areas target the Peri-LC dendritic area. For example, ventrolateral PAG exhibits a strong preference to the rostromedial Peri-LC (Ennis et al., 1991) and our data suggest that mPFC also preferentially targets this sub-region. Interestingly, two other forebrain structures, central nucleus of amygdala (CNA) and bed nucleus of stria terminalis (BNST), are also projecting to the rostral Peri-LC, but mainly in the rostrolateral Peri-LC rather than the rostromedial Peri-LC (Van Bockstaele et al., 1999, 2001). In addition, BNST and nucleus of solitary tract (NTS) are two nuclei which demonstrate a more defined topographic arrangement in the rostral Peri-LC. In particular, lateral part of the BNST and NTS target the rostrolateral Peri-LC, while the medial part of the BNST and NTS show the preference to the rostromedial Peri-LC (Van Bockstaele et al., 1999, 2001), suggesting a functional correlation between these two rostral dendritic areas, i.e., rostrolateral and rostromedial regions. Although caudal juxtaependymal Peri-LC is another major extranuclear peri-LC sub-region (Shipley et al., 1996), serotonergic DR may be the only known region showing the preference to this area. Projection patterns from ventral tegmental area (VTA), median raphe (MR) and spinal cord has yet to be elucidated.

Functionally, the diverse inputs to the LC have suggested that LC is not only a relay nucleus but also a site for polymodal integration. Irrespective of the broad projection from LC nucleus, previous study has also demonstrated a selective collateralization from the LC to the sensory system (Simpson et a., 1997). Thus, the highly selective afferent patterns to the LC may provide another mechanism or substrate which allows LC neurons to code, assimilate, and possibly prioritize converging streams of information to specific brain areas.

Acknowledgments

This research was supported by NIH grants RR017701 (KLS), EUREKA MH084194 (RCSL).

REFERENCE

Amodio DM, Frith C. Meeting of minds: the medial frontal cortex and social cognition. Nat neurosci. 2006; 7:268–277.

Amat J, Baratta MV, Paul E, Bland ST, Watkins LR, Maier SF. Medial prefrontal cortex determines how stressor controllability affect behavior and dorsal raphe nucleus. Nat Neurosci. 2005; 8(3):365–371. [PubMed: 15696163]

Arnsten AF, Goldman-Rakic PS. Selective prefrontal cortical projections to the region of the locus coeruleus and raphe nuclei in the Rhesus monkey. Brain Res. 1984; 306:9–18. [PubMed: 6466989]

Aston-Jones G, Ennis M, Pieribone VA, Nidkell VT, Shipley MT. The brain nucleus locus coeruleus: restricted afferent control of a broad efferent network. Science. 1986; 234:734–737. [PubMed: 3775363]

Aston-Jones G, Akaoka H, Charlety P, Chouvet G. Serotonin selectively attenuates glutamate-evoked activation of noradrenergic locus coeruleus neurons. J Neurosci. 1991; 11:760–769. [PubMed: 1672153]

Barnes CA, Pompeiano M. Neurobiology of the locus coeruleus. Prog Brain Res. 1991; 88:307–321. [PubMed: 1687619]

Blier P, DE Montigny C. Serotonergic neurons and 5-HT receptors in the CNS. Handbook of experimental pharmacology. 1997; 129:727–750.

Brown VJ, Bowman EM. Rodent models of prefrontal cortical function. Trends in Neurosci. 2002; 25(7):340–343.

Cedarbaum JM, Aghajanian GK. Afferent projections to locus coeruleus as determined by a retrograde tracing technique. J Neurol. 1978; 178:1–16.

Clark FM, Proudfit HK. The projection of locus Coeruleus neurons to the spinal cord in the rat determined by anterograde tracing combined with immunocytochemistry. Brain Res. 1991; 538:231–245. [PubMed: 2012966]

Damasio AR. Neuropsychology: Towards a neuropathology of emotion and mood. Nature. 1997; 386:769–770. [PubMed: 9126732]

Davidson RJ. Anxiety and affective style: role of prefrontal cortex and amygdale. Biol Psychiatry. 2002; 51(1):68–80. [PubMed: 11801232]

Doraiswamy PM, Varia I, Hellegers C, Wagner HR, Clary GL, Beyer JL, Newby LK, O'Connor JF, Beebe KL, O'Connor C, Drishnan KRR. A randomized controlled trial of paroxetine for noncardia chest pain. Psychopharmacol Bull. 2006; 39(1):15–24. [PubMed: 17065971]

Ennis M, Behbehani M, Shipley MT, Van Bockstaele EJ, Aston-jones G. Projections from the periaqueductal gray to the rostromedial pericoerulear region and nucleus locus coeruleus: Anatomic and physiology studies. J Comp Neurol. 1991; 306:480–494. [PubMed: 1713927]

Foote SL, Bloom FE, Aston-Jones G. Nucleus locus coeruleus: New evidence of anatomical and physiological specificity. Physiol Rev. 1983; 63:844–914. [PubMed: 6308694]

Goldman-Rakic PS. Cellular and circuit basis of working memory in prefrontal cortex of non-human primates. Prog Brain Res. 1990; 85:325–336. [PubMed: 2094903]

Hartman BK, Zide D, Udenfriend S. The use of dopamine-β-hydroxylase as a marker for the central noradrenergic nervous system in rat brain. Proc Nat Acad Sci USA. 1972; 69:2722–2726. [PubMed: 4560699]

Imai H, Steindler DA, Kitai ST. The organization of divergent axonal projections form the midbrain raphe nuclei in the rat. J Comp Neurol. 1986; 243:363–380. [PubMed: 2419370]

Jodo E, Aston-Jones G. Activation of locus coeruleus by prefrontal cortex is mediated by excitatory amino acid inputs. Brain Res. 1997; 768:327–332. [PubMed: 9369332]

Jodo E, Chaing C, Aston-Jones G. Potent excitatory influence of prefrontal cortex on noradrenergic locus coeruleus. Neurosci. 1998; 83:63–79.

Kim MA, Lee HS, Lee BY, Waterhouse BD. Reciprocal connections between subdivisions of the dorsal raphe and the nuclear core of the locus coeruleus in the rat. Brain Res. 2004; 1026:56–67. [PubMed: 15476697]

Lee HS, Kim MA, Waterhouse BD. Retrograde double-labeling study of common afferent projections to the dorsa raphe and the nuclear core of the locus coeruleus in the rat. J Comp Neurol. 2005; 481:179–193. [PubMed: 15562508]

Loughlin SE, Foote SL, Fallon JH. Locus coeruleus projections to cortex: Topography, morphology and collateralization. Brain Res Bul. 1982; 9(1-6):287–294.

Luppi PH, Aston-Jones G, Akaoka H, Chouvet G, Jouvet M. Afferent projections to the rat locus coeruleus demonstrated by retrograde and anterograde tracing with cholera-toxin B subunit and Phaseolus vulgaris leucoagglutinin. Neurosci. 1995; 65:119–160.

Maciag D, Simpson KL, Coppinger D, Lu Y, Wang Y, Lin RCS, Paul IA. Neonatal antidepressant exposure has lasting effects on behavior and serotonin circuitry. Neuropsychopharmaco. 2006; 31:47–57.

Mason ST, Fibiger HC. Regional topography within noradrenergic locus coeruleus as revealed by retrograde transport of horseradish peroxides. J Comp Neurol. 1979; 187:703–724. [PubMed: 90684]

McRae-Deguerce A, Milon H. Serotonin and dopamine afferents to the rat locus coeruleus: a biochemical study after lesioning of the ventral mesencephalic tegmental-A 10 region and the raphe dorsalis. Brain Res. 1983; 263:344–347. [PubMed: 6301650]

Nance DM, Burns J. Fluorescent dextrans as sensitive anterograde neuroanatomical tracers: application and pitfalls. Brain Res Bull. 1990; 25(1):139–145. [PubMed: 1698517]

Owern MJ, Nemeroff CB. Role of serotonin in the pathophysiology of depression: focus on the serotonin transporter. Clin Chem 40. 1994; 2:288–295.

Paxinos, G.; Watson, C. The rat brain in stereotaxic coordinates. second edition. Academic press; Sydney: 1986.

Proudfit HK, Clark FM. The projection of locus Coeruleus neurons to the spinal cord. Prog Brain Res. 1991; 88:123–141. [PubMed: 1813919]

Radley JJ, Arias CM, Sawchenko PE. Regional differentiation of the medial prefrontal cortex in regulating adaptive responses to acute emotional stress. J Neurosci. 2006; 13(50):12967–12976. 26. [PubMed: 17167086]

Ressler KJ, Nemeroff CB. Role of serotonergic and noradrenergic systems in the pathophysiology of depression and anxiety disorders. Depress Anxiety. 2000; 12:2–19. [PubMed: 11098410]

Rosenkilde CE. Functions of the prefrontal cortex: Behavioral investigations using ablation and electrophysiological techniques in rats, cats, dogs, and monkeys. Acta Physiol Scand [Suppl]. 1983; 514:4–58.

Rouzade-Dominguez ML, Curtis AL, Valentino RJ. Role of Barrington's nucleus in the activation of rat locus Coeruleus neurons by colonic distension. Brain Res. 2001; 917:206–218. [PubMed: 11640906]

Segal M. Serotonergic innervation of the locus coeruleus from the dorsal raphe and its action on responses to noxious stimuli. J Physiol. 1979; 286:401–415. [PubMed: 439032]

Segal M, Sanderg M. Analgesia produced by electrical stimulation of catecholamine nuclei in the rat brain. Brain Res. 1977; 123:369–372. [PubMed: 843931]

Sesack SR, Deutch AY, Roth RH, Bunney BS. Topographical organization of the efferent projection of the medial prefrontal cortex in the rat: An anterograde tract tracing study with Phaseolus Vulgaris Leucoagglutinin. J Comp Neurol. 1989; 290:213–242. [PubMed: 2592611]

Shimodozono M, Kawahira K, Kamishita T, Ogata A, Tohgo S, Tanaka N. Reduction of central poststroke pain with the selective serotonin reuptake inhibitor fluvoxamine. J Neurosci. 2002; 112(10):1173–1181.

Shipley MT, Fu L, Ennis M, Liu WL, Aston-Jones G. Dendrites of locus coeruleus neurons extend preferentially into two pericoerulear zones. J Comp Neurol. 1996; 365:56–68. [PubMed: 8821441]

Simpson KL, Altman DW, Wang L, Kirifides KL, Lin RCS, Waterhouse BD. Lateralization and functional organization of the locus coeruleus projection to the trigeminal somatosensory pathway in rat. J Comp Neurol. 1997; 385:135–147. [PubMed: 9268121]

Simpson, KL.; Lin, RCS. Neuroanatomical and chemical organization of the locus coeruleus.. In: Ordway, GA.; Schwartz, MA.; Frazer, A., editors. Brain norepinephrine: Neurobiology and Therapeutics. Cambridge University Press; 2007. p. 9-52.

Swanson LW, Hartman BK. The central adrenergic system: an immunofluorescence study of the location of cell bodies and their efferent connections in the rat utilizing dopamine-β-hydroxylase as a marker. J Comp Neurol. 1975; 163:467–505. [PubMed: 1100685]

Swanson LW. An autoradiographic study of the efferent connections of the preoptic region in the rat. J Comp Neurol. 1976a; 167:227–256. [PubMed: 819466]

Swanson LW. The locus coeruleus: a cytoarchitectonic, Golgi and immunhistochemical study in the albino rat. Brain Res. 1976b; 110:39–56. [PubMed: 776360]

Szabo ST, Blier P. Serotonin (1A) receptors ligands act on norepinephrine neuron firing through excitatory amino acid and GABA (A) receptors: A microiontophoretic study in the rat locus coeruleus. Synapse 15. 2001; 42:203–212.

Szabo ST, DE Montigny C, Blier P. Modulation of noradrenergic neuronal firing by selective serotonin reuptake blockers. Bri J Pharmacol. 1999; 126:568–571.

Talley NJ. How effective is fluoxetine for the treatment of pain and constipation-predominant irritable bowel syndrome? Nat Clin Pract Gastroenterol Hepatolo. 2006; 3:196–197.

Valentino RJ, Chen S, Zhu Y, Aston-Jones G. Evidence for divergent projections to the brain noradrenergic system and the spinal parasympathetic system from Barrington's nucleus. Brain Res. 1996; 732:1–15. [PubMed: 8891263]

Van Boskstaele EJ, Peoples J, Telegan P. Efferent projections of the nucleus of the solitary tract to peri-locus Coeruleus dendrites in rat brain: evidence for a monosynaptic pathway. J Comp Neurol. 1999; 412:410–428. [PubMed: 10441230]

Van Boskstaele EJ, Bajic D, Proudfit H, Valentino RJ. Topographic architecture of stress-related pathways targeting the noradrenergic locus Coeruleus. Physiol Behav. 2001; 73:273–283. [PubMed: 11438352]

Vercelli A, Repici M, Garbossa D, Grimaldi A. Recent techniques for tracing pathways in the central nervous system of developing and adult mammals. Brain Res Bull. 2000; 51(1):11–28. [PubMed: 10654576]

Vertes RP, Kocsis B. Projections of the dorsal raphe nucleus to the brainstem: PHA-L analysis in the rat. J Comp Neurol. 1994; 340:11–26. [PubMed: 8176000]

Weaver KJ, Paul IA, Lin RCS, Simpson KL. Neonatal exposure to citalopram selectively alters the expression of the serotonin transporter in the hippocampus: dose-dependent effects. Anat Rec. 2010; 293:1920–1932.

Xu YL, Sari Y, Zhou FC. Selective serotonin reuptake inhibitor disrupts organization of thalamocortical somatosensory barrels during development. Dev Brain Res. 2004; 150:151–161. [PubMed: 15158078]

Zhang JL, Darling RD, Paul IA, Simpson KL, Chen K, Shih JC, Lin RCS. Altered expression of Tyrosine hydroxylase in the Locus coeruleus noradrenergic system in citalopram neonatally exposed rats and monoamine oxidase A knock out mic. Anat Rec. 2011; 294:1685–1697.

Zhou FC, Xu Y, Bledsoe S, Lin R, Kelly MR. Serotonin transporter antibodies: production, characterization, and localization in the brain. Mol Brain Res. 1996; 43:267–278. [PubMed: 9037542]

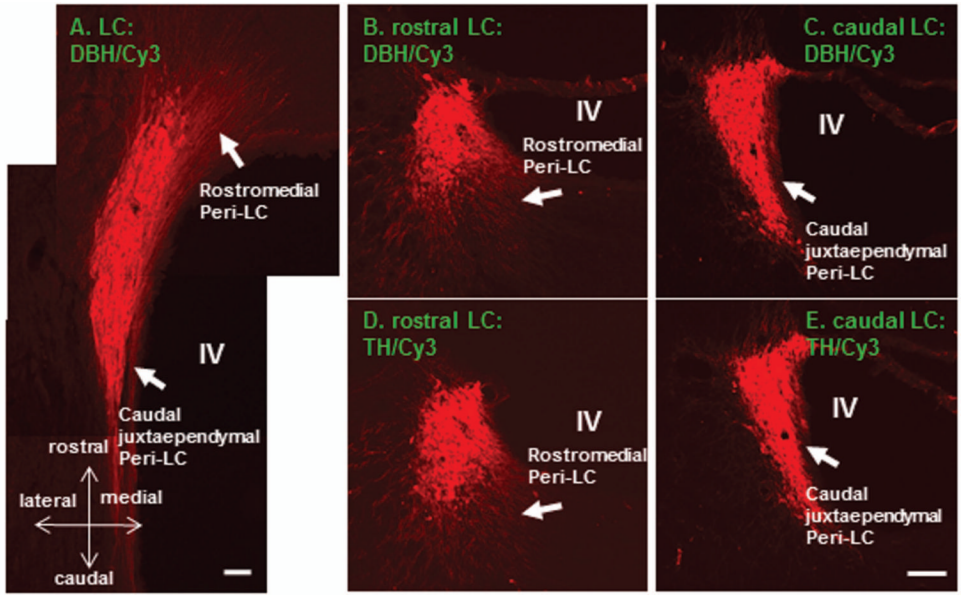

Figure 1.

Color photomicrographs illustrate DBH or TH immunoreactive profiles in the LC (A-E; Cy3: red). It is quite obvious that DBH and TH immunoreactivity in the adjacent sections revealing highly similar labeling patterns (B-E). Extranuclear LC processes are mainly noted in the rostromedial and caudal juxtaependymal Peri-LC. These two subregions are marked in B-E (arrows) and also are clearly visualized in the horizontal section (A). DBH: dopamine-beta-hydroxylase; TH: tyrosine hydroxylase; LC: locus coeruleus; IV: the IVth ventricle. Scale bar: 80 μm.

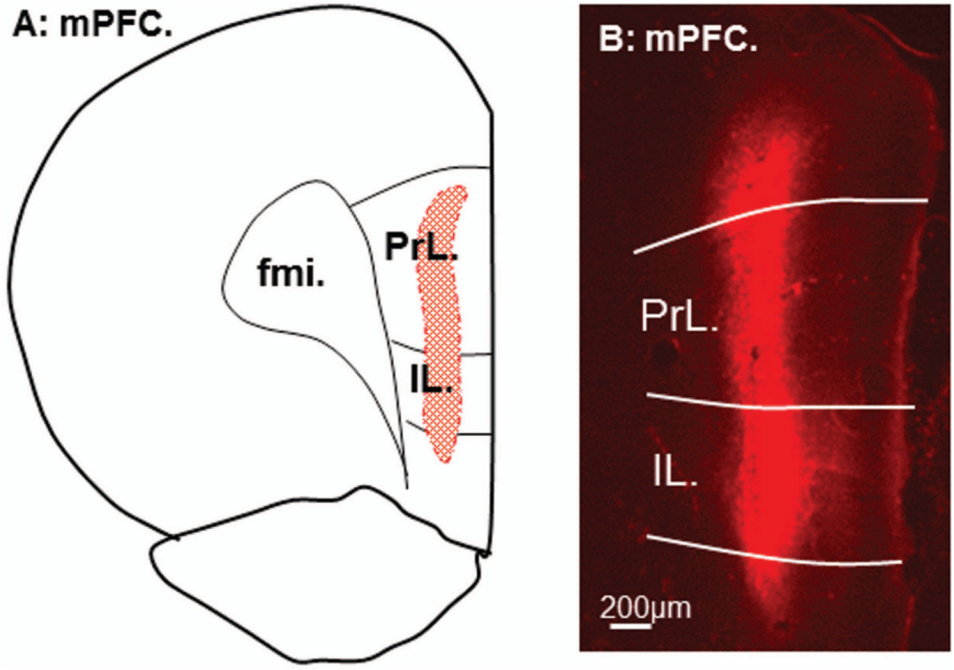

Figure 2.
Line drawing from reconstruction of anterograde tracer fluoro-ruby (FR) injection site in the mPFC is shown in A. A representative of FR (red) injection site is shown in B. Note that the spread of the tracer is restricted within the mPFC. PrL: prelimbic cortex; IL: infralimbic cortex; fmi: forceps minor of corpus callosum; mPFC: medial prefrontal cortex.

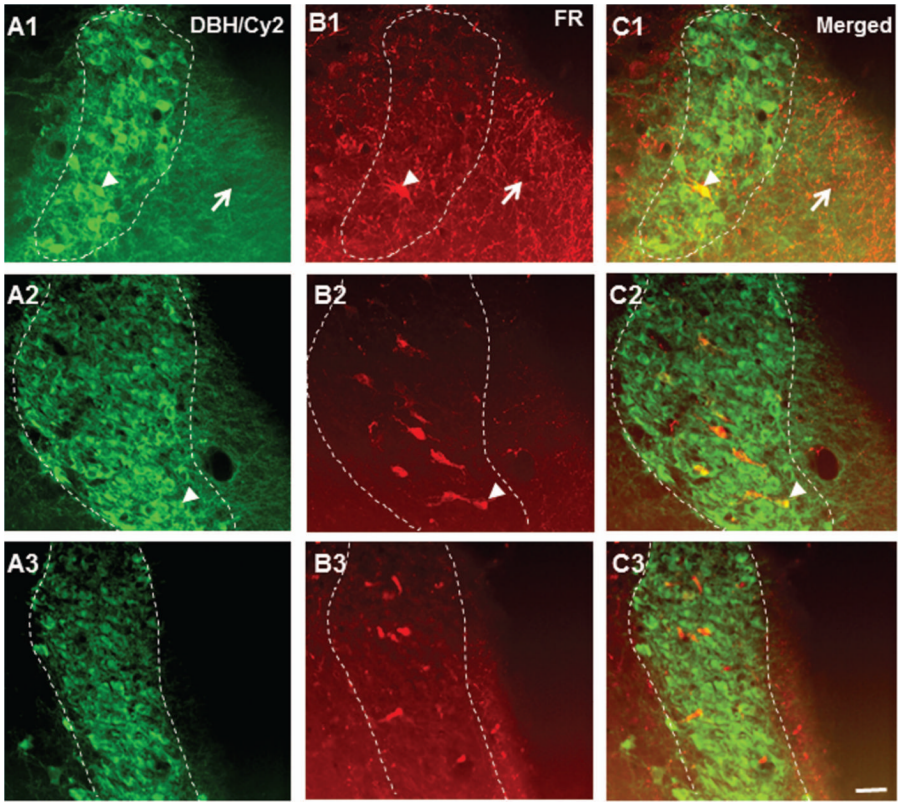

Figure 3.

Color photomicrographs demonstrate the spatial relationship between mPFC-LC projecting fibers and DBH labeled LC (circled by dashed lines) in coronal sections. The left column shows DBH labeled LC profiles from rostral to caudal (A1-A3; Cy2: green). The middle column exhibits FR anterogradely labeled mPFC-LC projecting fibers and also a few FR retrogradely LC-mPFC projection neurons (B1-B3; red). The right column shows the merged photos. Note that the majority of mPFC-LC projecting fibers are located in the rostral sector of the LC, especially the rostromedial Peri-LC (marked by arrows in upper row), and very few fibers can be identified in the intermediate and caudal levels. In addition, a few FR labeled LC-mPFC projection neurons are noticed throughout all LC levels (marked by arrow heads). Scale bar: 30 μm.

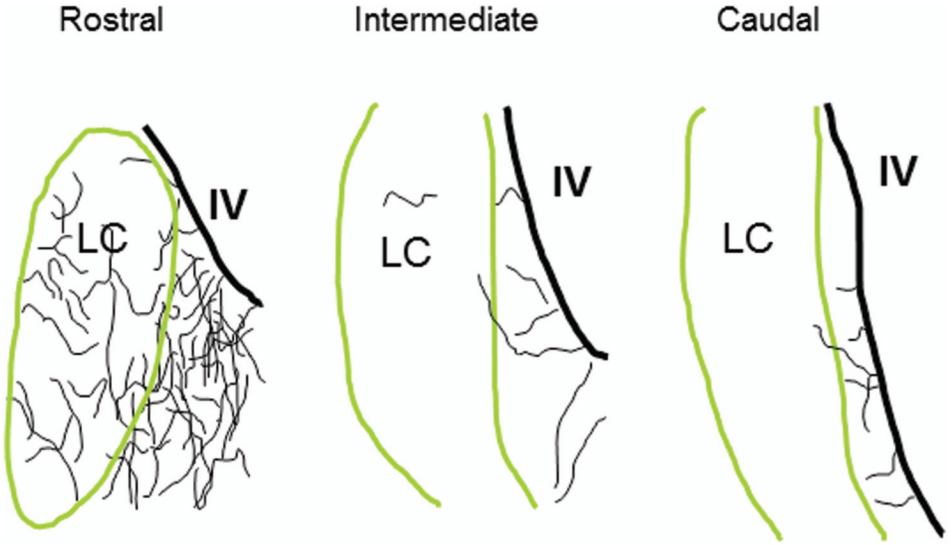

Figure 4.

Schematic line drawings illustrate the spatial relationship between mPFC-LC projecting fibers and LC nuclear core vs Peri-LC dendritic zones. Note that mPFC-LC descending fibers are mainly situated in the rostral sector of the LC, especially the rostromedial Peri-LC. LC: locus coeruleus; IV: 4th ventricle.

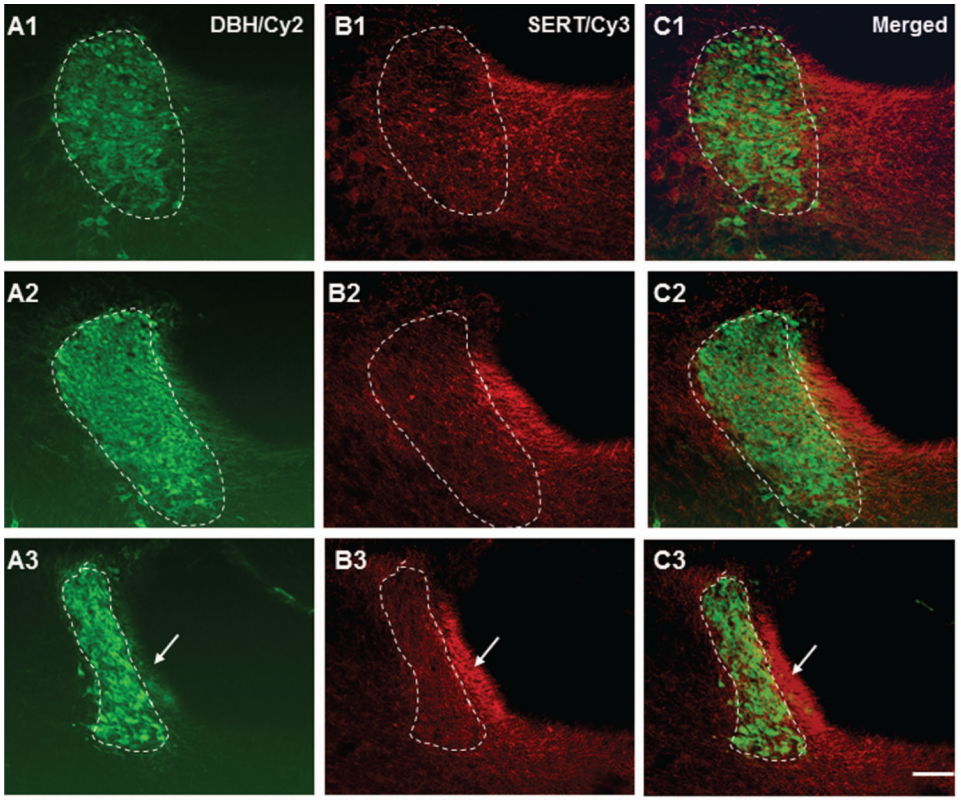

Figure 5.

Color photomicrographs demonstrate the spatial relationship between serotonin transporter (SERT) immunoreactive fibers and DBH positive LC nucleus (circled by dashed lines). The left column shows the LC from rostral to caudal (A1-A3) immunostained with DBH antiserum (Cy2: green). The middle column reveals SERT positive fibers from the same section (A2-C2; Cy3: red). The right column shows the merged photos. Note that SERT positive fibers are rather prevalent in the caudal juxtaependymal Peri-LC (marked by arrows in lower row). Scale bar: 60 μm.

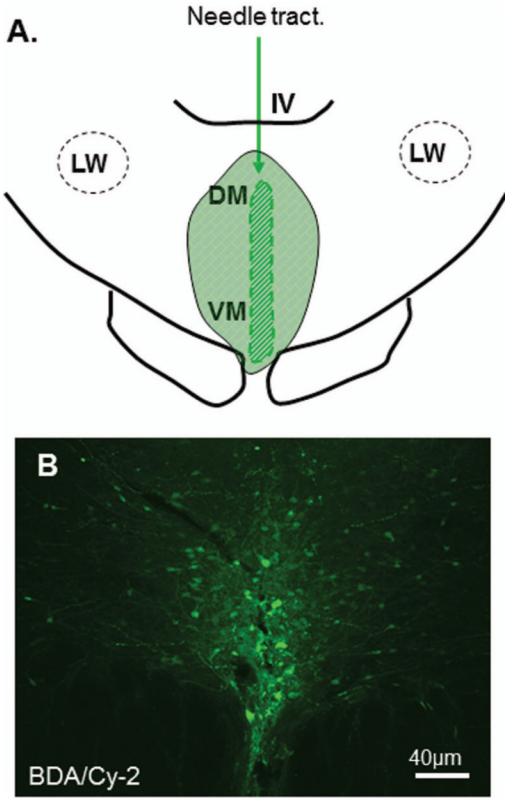

Figure 6.
Line drawing for the reconstruction of anterograde tracer injection site in the DR is shown in A. The fluorescent stained BDA (Cy2: green) reaction reveals the injection site in the DR (B). Note that a majority of BDA labeled cells are restricted in the DR. IV: 4th ventricle; LW: lateral wing; DM: dorsomedial; VM: ventromedial.

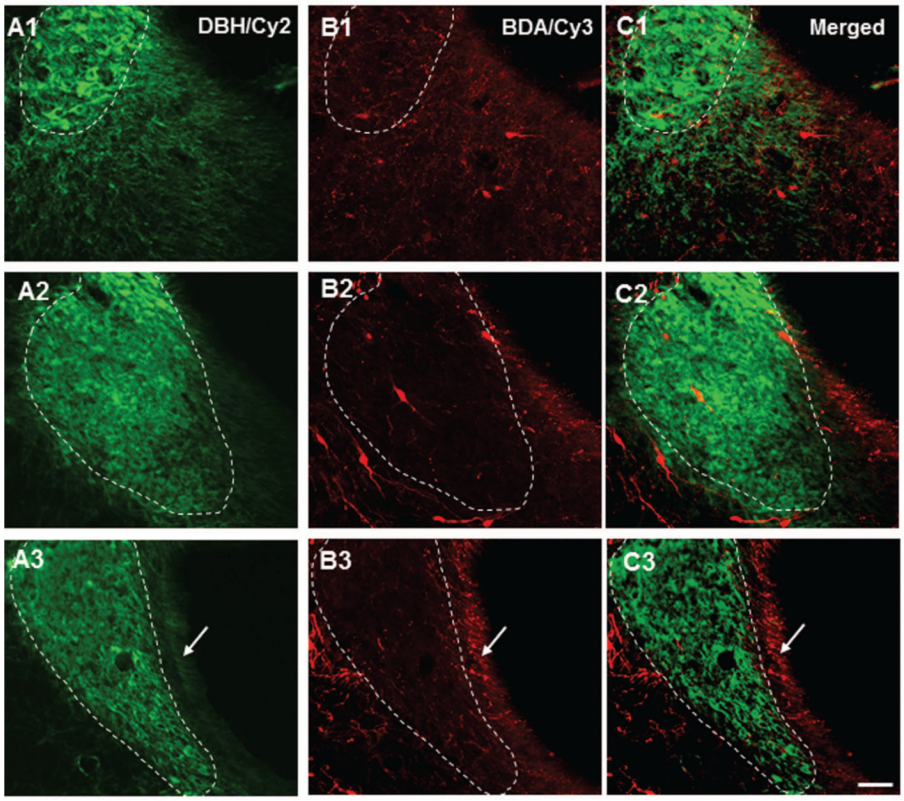

Figure 7.
Color photomicrographs demonstrate the spatial relationship between DR-LC projecting fibers and DBH immunoreactive LC nucleus (circled by dashed lines). The left column shows LC profiles from rostral to caudal to reveal DBH immunostaining pattern (A1-A3; Cy2: green). The middle column reveals BDA anterogradely labeled DR-LC projecting fibers in the LC (B1-B3; Cy3: red). The right column shows the merged photos. The arrows point to the caudal juxtaependymal Peri-LC which contains the highest density of DR-LC projecting fibers. Scale bar: 40 μm.

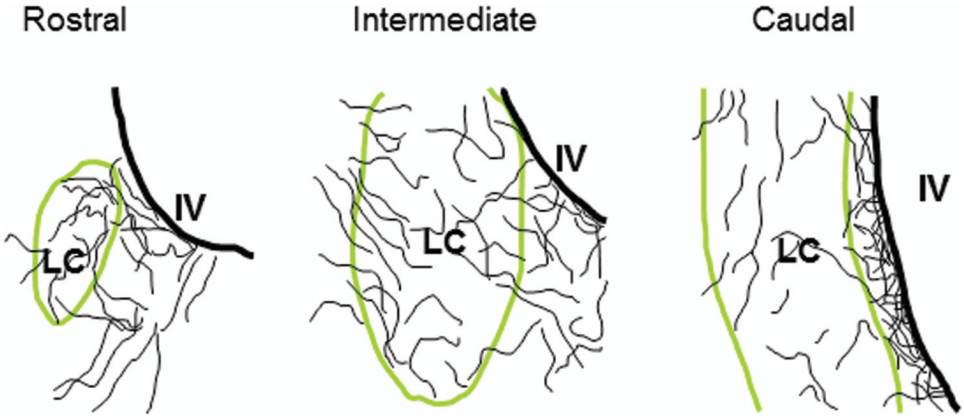

Figure 8.
Schematic line drawings illustrate the spatial relationship between DR-LC projecting fibers and LC nuclear core vs Peri-LC. Note that anterogradely labeled DR-LC projecting fibers exhibit a preference to the caudal juxtaependymal Peri-LC. LC: locus coeruleus; IV: 4th ventricle.

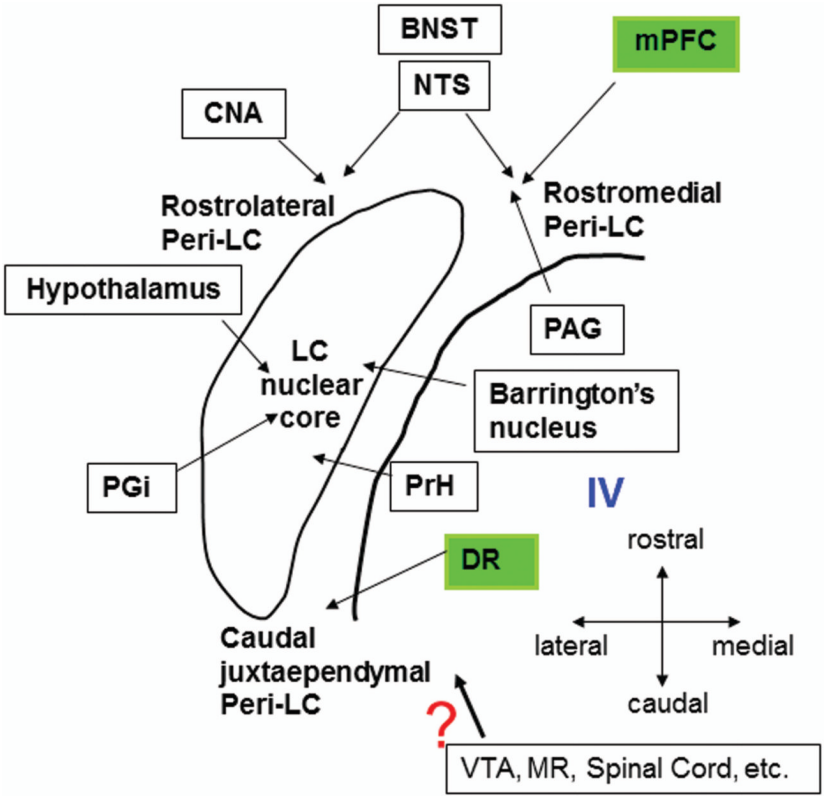

Figure 9.

Schematic diagram summarizes the overall topography of known afferent inputs to the LC. The area enclosed within the thin line denotes the LC nuclear core in the horizontal plane. Note that rostral Peri-LC tends to receive innervation from medial prefrontal cortex (mPFC), bed nucleus of stria terminals (BNST), central nucleus of amygdala (CNA), nucleus of solitary tract (NTS) and ventrolateral periaqueductal area (PAG). While mPFC and PAG mainly target the rostromedial Peri-LC, and CNA mainly targets the rostrolateral Peri-LC as well as BNST and NTS project to both rostromedial and rostrolateral Peri-LC. In contrast, DR is the only known structure to exhibit a preference to the caudal juxtaependymal Peri-LC. Additionally, nucleus paragigantocellularis (PGi), nucleus prepositus hypoglossi (PrH), Barrington's nucleus and the paraventricular nucleus of the hypothalamus appear to preferentially target the LC nuclear core. The precise distribution of afferents arising from other regions such as ventral tegmental area (VTA), median raphe (MR) and spinal cord etc. has yet to be determined. IV: 4th ventricle. (the drawing is modified from Simpson and Lin, 2007).